Biosensors and Bioelectronics 26 (2011) 1883–1889

Contents lists available at ScienceDirect

Biosensors and Bioelectronics

journal homepage: www.elsevier.com/locate/bios

Development of an acetaminophen amperometric biosensor based on peroxidase entrapped in polyacrylamide microgels

M.I. González-Sánchez[a,1], J. Rubio-Retama[b,2], E. López-Cabarcos[b,2], E. Valero[a,*]

[a] Departamento de Química-Física, Escuela de Ingenieros Industriales, Universidad de Castilla-La Mancha, Campus Universitario, 02071 Albacete, Spain
[b] Departamento de Química-Física II, Facultad de Farmacia, Universidad Complutense de Madrid, 28040 Madrid, Spain

ARTICLE INFO

Article history:
Received 10 December 2009
Received in revised form 18 March 2010
Accepted 18 March 2010
Available online 25 March 2010

Keywords:
Enzymatic biosensor
Horseradish peroxidase
Polyacrylamide microgels
Acetaminophen
Hill equation
Diffusion coefficients

ABSTRACT

In this work, horseradish peroxidase (HRP) has been entrapped in cross-linked polyacrylamide microparticles using the concentrated emulsion polymerization method. The feasibility of amperometric detection of acetaminophen (APAP) in a biosensor using this HRP immobilized system as the biological material in the presence of hydrogen peroxide was investigated. We found that the optimum microgel cross-linking degree required to retain the protein and to allow the diffusion of the phenolic drug onto the microparticles was 8%. The apparent diffusion coefficients of APAP across the different microparticles have been calculated using the Cottrell equation. The diffusion coefficients decrease as the microgel cross-linking increases, and the data fit an uniexponential equation well. Those microparticles with a cross-linking degree lower than 5% operated under kinetic control, whereas those whose cross-linking degree was above this value operated under diffusion control. Biosensor response was also optimized to investigate the effect of H_2O_2 concentration and enzyme loading on the current intensity. Under optimal conditions, the sensitivity of this biosensor for APAP was 74.9 mA M^{-1} cm^{-2}, the detection limit was 3.1×10^{-6} M based on S/N = 3 and the response time was 135 s. The linear range goes from 1.0×10^{-5} to 4.9×10^{-4} M APAP, and can be extended using the Hill equation to 5.7×10^{-3} M. The biosensor is selective for APAP and was applied to determine the APAP concentration in three commercial pharmaceutical formulations.

1. Introduction

APAP (4′-hydroxyacetanilide, paracetamol) is one of the world's most widely used nonprescription medicines. Although therapeutic doses of the drug are reported to be safe, overdoses cause centrilobular hepatic necrosis that can be fatal in both humans and laboratory animals (Josephy, 2005). APAP overdoses account for more than 56,000 emergency room visits, 2600 hospitalizations and an estimated 458 acute liver failures each year in the United States (Lee, 2007). Because of this high incidence of APAP poisoning cases, ongoing research efforts have been made to understand APAP hepatotoxicity mechanisms and to develop new specific methods for measuring the drug in pharmaceutical formulations and biological fluids. Spectrophotometry (Mohamed et al., 1997), liquid chromatography (Marin et al., 2002), capillary electrophoresis (Zhao et al., 2006), chemiluminescence (Easwaramoorthy et al., 2001) and FTIR and Raman spectrometry (Al-Zoubi et al., 2002) have been effectively used for the determination of APAP in blood and pharmaceutical preparations. However, these methods have some disadvantages such as high costs, long analysis times and the need for sample pre-treatment, and even low sensitivity and selectivity in some cases, thus rendering them unsuitable for routine analyses. Table 1S (Supplementary information) shows sensitivity, linearity and time-of-analysis data for the above references. For a more extensive review about acetaminophen determination see Espinosa-Bosch et al. (2006).

Enzymatic biosensors are an attractive alternative for APAP determination given their specifity, precision, and ease and speed of use. Different enzymes have been used in the design of biosensors for the quantitative analysis of APAP. Thus, an amperometric biosensor based on aryl acylamidase (aryl-acylamide amidohydrolase, EC 3.5.1.13) for the rapid APAP determination in whole blood was first developed (Vaughan et al., 1991). However, this enzyme is not commercially available among the usual distributors. Tyrosinase (monophenol, o-diphenol: oxygen oxidoreductase, EC 1.14.18.1) has also been used in the design of a biosensor based on vaseline-graphite modified with avocado tissue as the source of the enzyme for chronoamperometric APAP

* Corresponding author. Tel.: +34 967 59 92 00; fax: +34 967 59 92 24.
E-mail addresses: MIsabel.Gonzalez@uclm.es (M.I. González-Sánchez), bjrubio@farm.ucm.es (J. Rubio-Retama), cabarcos@farm.ucm.es (E. López-Cabarcos), Edelmira.Valero@uclm.es (E. Valero).
[1] Tel.: +34 967 59 92 00; fax: +34 967 59 92 24.
[2] Tel.: +34 913 94 17 50; fax: +34 913 94 20 32.

0956-5663/$ – see front matter © 2010 Elsevier B.V. All rights reserved.
doi:10.1016/j.bios.2010.03.024

determination in pharmaceutical formulations (Fatibello et al., 2001). The drawback of using this enzyme is that it shows complex kinetics towards monophenols like APAP, displaying a lag phase in progress curves (Valero et al., 2002). This results in long response times of tyrosinase-based sensors towards monophenols (Hervás-Pérez et al., 2006), although the lag period could be shortened by the addition of a nucleophilic agent (Valero et al., 2003a,b). An alternative approach is the use of HRP (donor: hydrogen peroxide oxidoreductase, EC 1.11.1.7) for APAP biosensors design in the presence of hydrogen peroxide. HRP catalyzes the one-electron oxidation in the presence of H_2O_2 of APAP to the radical species N-acetyl-*p*-benzosemiquinone imine (NAPSQI•), as shown by ESR studies (Bessems et al., 1998). A scheme of the catalytic cycle of HRP towards APAP can be seen in Fig. 1S (Supplementary information).

HRP-based amperometric biosensors have already been described for the investigation of drug compounds (Harwood and Pouton, 1996; Alonso-Lomillo et al., 2003) and many different approaches can be found in the literature. In the particular case of APAP, a continuous flow sensing device with an HRP-modified pre-cell coupled to an amperometric detector was developed for monitoring the drug in pharmaceutical formulations (Messina et al., 2006), but the current response was quite low. Other authors have used HRP immobilized onto nanoporous magnetic silica microparticles for APAP biotransformation and inhibition studies (Yu et al., 2006), but the inconvenience of this approach is its limited enzymatic load. HRP has also been adsorbed in a polyethyleneimine and zirconium alcoxide porous gel film for APAP detection (Sima et al., 2008), although protein desorption is a drawback of this method as a result of the weakness of the bonds involved. In addition these reports erroneously indicate that the product of the reaction is N-acetyl-*p*-benzoquinone imine (two-electron oxidation) which does not correspond to HRP-mechanism (one-electron oxidation).

Polyacrylamide (PAA) gels have been used as a matrix for electrophoresis, as a support for enzyme and drug encapsulation, and more recently as an enzyme immobilization system for biosensors design (Rubio-Retama et al., 2003). Monoenzyme biosensors with glucose oxidase (Rubio-Retama et al., 2005), tyrosinase (Hervás-Pérez et al., 2006) and choline oxidase (Sánchez-Paniagua López et al., 2007) entrapped in PAA microgels have been reported. These reports show that numerous advantages (stability, reproducibility, repeatibility, etc.) can be achieved in the fabrication of new enzyme biosensors with these materials. However as far as we are aware, no studies about the encapsulation of HRP in PAA microparticles have been reported. Therefore the aim of the present paper was to develop an amperometric biosensor based on HRP entrapped within PAA microparticles as a biological component. Of special interest are the high stability of HRP-PAA microencapsulated, the simplicity of both the microparticles and biosensor preparation, and high specificity. Experimental variables such as the amount of cross-linker used for the HRP encapsulation, H_2O_2 concentration and enzymatic load have been optimized, thus enabling measurement under the best conditions. Diffusion coefficients have also been calculated to further evaluate the diffusion limitations inside microparticles.

2. Materials and methods

2.1. Chemical and buffers

APAP, L-ascorbic acid, citric acid, salicylic acid, caffeine, D-mannitol, D-(+)-glucose, acrylamide (AA), N,N′-methylenebisacrylamide (BIS), dodecane and HRP (167 units/mg solid) were purchased from Sigma (St. Louis, MO, USA). Ammonium persulfate, N,N,N′,N′-tetramethylenediamine (TEMED), Span 80 and H_2O_2 were from Fluka (Madrid, Spain). All the other reagents were of analytical grade and were used without further purification. The dialysis membrane (12,000–14,000 MWCO) was purchased from Spectrum Medical Industries. Solutions were prepared with demineralized water purified through a Milli-Q purification system (18.2 MΩ cm) (Millipore Corp., Bedford, MA). Unless otherwise specified, all the solutions were prepared using 50 mM sodium phosphate buffer (PBS) pH 7.0 with 0.1 M KCl as a supporting electrolyte.

Commercial medicines of three different brands containing APAP as the active component were purchased in a local pharmacy. Their declared doses are 650 (Termalgin and Cinfa; samples nos. 1 and 2, respectively) and 500 mg/tablet (Winthrop, sample no. 3). Commercial APAP stock solutions were prepared for each brand as follows: 5 tablets of each trademark were weighed and ground to a fine powder in three different mortars; an amount equivalent to 2 tablets was dissolved in 150 ml of PBS for each trademark. After 2 h of mechanical shaking, solutions were filtered through a 0.22 μm filter. Residues were washed three times with 25 ml of buffer and brought to 250 ml in calibrated flasks. At the end of this process, three stock solutions with the following expected APAP concentrations were obtained: 34.4 mM (samples nos. 1 and 2) and 26.5 mM (sample no. 3).

2.2. Synthesis of microgels with entrapped HRP

PAA microparticles with increasing amounts of BIS as cross-linker and HRP entrapped were prepared using the concentrated emulsion polymerization method (Rubio-Retama et al., 2003). The amount of cross-linker, η, given as the ratio between the weight of the cross-linker (BIS) and the monomer (AA), varied between 3% and 9%. The encapsulation of HRP was carried out by solubilizing the enzyme in PBS pH 7.0, which constitutes the dispersed aqueous phase. W/O concentrated emulsions were produced by dropwise addition of the dispersed phase to the continuous oil phase (Dodecane plus Span 80). Redox polymerization of the gel-like emulsion produced entrapped enzyme microgels. Temperature was controlled and kept below 35 °C during polymerization to maintain enzyme activity and to avoid protein denaturation. Microparticles were washed and centrifuged several times until no enzymatic activity was observed in the supernatant. This protocol generated PAA microparticles with diameters of between 1 μm and 32 μm.

The microgel particles were examined using scanning electron micrographs (SEM) with a JEOL JSM-6400 microscope (JEOL, Japan) operating at an acceleration voltage of 20 kV and with 5000 magnification. For studying the size distribution, freeze-dried microgels were dispersed in water for 24 h and observed with an optical microscope. Four hundred particles were picked up randomly from optical microscope photographs, and their diameters were measured using the UTHSCSA ImageTool (V.3.0) to calculate the average diameter and the size distribution of the microgels prepared with different cross-linker concentrations.

2.3. Electrode preparation

The glassy-carbon electrode surface was polished with 0.05 μm alumina slurry paste, and any residual abrasive particles were ultrasonically removed in methanol and distilled water. Afterwards the electrode was pretreated by applying a potential of +1.8 V for 20 s in 0.1 M NaOH *vs.* Ag/AgCl (3 M KCl). An accurately weighed amount of microgel was placed on the working electrode surface and covered with the dialysis membrane. This membrane was attached with the aid of a thread. The resulting electrode was washed with 50 mM PBS pH 7.0 and a potential of −0.1 V *vs.* Ag/AgCl (3 M KCl) was applied until the background current dropped to a constant level.

2.4. Spectrophotometric assays

Spectrophotometric assays were performed with a UV/vis scanning spectrophotometer Uvikon 940 (Konton Instruments, Zürich, Switzerland). Temperature was controlled at 25 °C using a Hetofrig Selecta circulating bath with a heater/cooler and checked with a Checktemp 1 pocket digital thermometer obtained from Hanna Instruments with a resolution of 0.1 °C. The H_2O_2 concentration in the stock solutions was spectrophotometrically determined at 240 nm using a molar extinction coefficient of 39.5 M^{-1} cm^{-1} (Nelson and Kiesow, 1972). The APAP concentration was spectrophotometrically determined at 240 nm using a molar extinction coefficient of 9.7×10^3 M^{-1} cm^{-1} (González-Sánchez et al., 2009).

2.5. HPLC analysis

The APAP concentration in the pharmacological samples was measured in an Agilent Technologies (Waldbronn, Germany) HPLC system which was equipped with a series 1200 quaternary pump, a vacuum degasser and a diode array detector. Separations were performed on a reversed phase 5 μm Discovery C_{18} (15 cm × 4.6 mm) from Supelco (Madrid, Spain). Samples were filtered through a 0.45 μm filter prior to injection. Metabolites were eluted using a binary solvent system: a mixture of 2.8% (v/v) acetic acid in water and methanol (95:5). Solvents were previously filtered through a 0.22 μm filter and degassed by sonication in a Selecta Ultrasons water bath. The elution conditions were as follows: flow rate, 1.0 ml/min; injection volume, 20 μl and oven temperature 30 °C. Elution was monitored at 250 nm. Calibration straight lines for APAP were performed by duplicated injections of known amounts of it (0.1–1.0 mM). An Agilent ChemStation B.03.01 revision was used to integrate peak areas.

2.6. Amperometric measurements

Amperometric measurements were carried out using an Autolab potenciostat, Model PGSTAT302N (Eco Chemie B.V., The Netherlands). The system was run by PC via the General Purpose Electrochemical System software for Windows, version 4.9. All the electrochemical measurements were carried out in a three-electrode thermostated cell at 25 °C with a glassy-carbon electrode as the working electrode (with a surface area of 0.0314 cm^2), a Pt counter electrode and an Ag/AgCl (3 M KCl) electrode as a reference. The cell was protected from external electrical fields by a Faraday cage.

Steady-state amperometric measurements were made as follows: the electrode was immersed in the aqueous solution and subjected to a voltage of −0.1 V *vs.* SCE. When the recorder signal attained a stable value, a known volume of a standard APAP solution was added with constant stirring. Subsequently, the signal variation corresponding to the reduction of the enzymatically produced NAPSQI• was recorded. Calibration plots were made by successive additions of small volumes of a standard aqueous APAP solution in the presence of H_2O_2 at the indicated concentrations.

Apparent diffusion coefficients of APAP (D^{app}_{APAP}) for the different microgels used herein were calculated by a chronoamperometric method in an unstirred solution. A potential step of 0.6 V was applied to different bulk concentrations of APAP (5.0, 12.5 and 25.0 mM). At this potential value, APAP is irreversibly oxidized at the electrode surface, thus the APAP concentration in the electrode surface remains at zero. The standby potential was 0 and the equilibration time was 4 s. The response to the potential step of the blank solution was also recorded and the signal was subtracted from the APAP measurements. The number of electrons implicated in the direct oxidation of APAP at this potential value was considered to be 2 (Messina et al., 2006; Miner et al., 1981; Wangfuengkanagul and Chailapakul, 2002). The diffusion coefficients were calculated from the slope of a plot of I *vs.* $t^{-1/2}$ using the Cottrell equation (Bard and Faulkner, 2001). These experiments were performed in the absence of H_2O_2.

3. Results and discussion

3.1. Effect of cross-linking degree

HRP was entrapped in PAA microgels with different η to estimate the optimal pore size required for its immobilization. As η decreases, the pore size in the microgels becomes higher, so the amount of water entrapped into PAA microparticles also increases, leading to a greater degree of swelling (Rubio-Retama et al., 2003). This fact can affect the activity of the entrapped enzyme. Fig. 1A and B shows the biosensor response against bulk APAP concentrations for η varied from 3% to 9%.

The maximum response (J_{max}) was obtained at η = 8% (see Table 2S in the Supplementary information). So this cross-linking degree value was selected for further experiments in this work (size distribution and an SEM micrograph of microparticles with η = 8% can be seen in Fig. 2S, Supplementary information). The decrease observed in J_{max} at a low η is attributed to the leakage of the enzyme due to the large pore size of these microgels since HRP is a small protein (MW = 40 kDa) (Barman, 1969). In fact, greater enzymatic activity was observed in the supernatants deriving from washing the microgels prepared with a low η. Conversely, the decrease of J_{max} observed at η = 9% is attributed to the diffusional barrier that appeared for the substrate and product resulting from the reduced pore size in the high cross-linked microgels.

3.2. Effect of H_2O_2 concentration

It is worth investigating how the H_2O_2 concentration affects the biosensor response since it acts as a suicide substrate towards heme proteins (Arnao et al., 1990; Nazari et al., 2009). The current decreased as the concentration of H_2O_2 increased for all microparticles, whatever their η (see Table 2S in the Supplementary information), which can be related to the H_2O_2-induced inactivation of HRP. However, the response of the electrode worsened when the H_2O_2 concentration dropped below 6.5 mM at the higher APAP concentrations (data not shown). So this particular concentration of H_2O_2 was chosen for further experiments.

3.3. Effect of the enzymatic load

The influence of the enzymatic load was examined by varying the amount of microparticles placed on the electrode surface (Fig. 1C). The current response was higher when the amount of the microparticles increased; the drawback involved was that the response time also increased (around 135 and 650 s for 1 and 3 mg of microparticles, respectively). As the response obtained for 1 mg of microparticles presented a good compromise between the current response and the response time, this value was chosen for further kinetic studies. Furthermore, it must be taken into account that the deviations from Michaelian behaviour were more pronounced when the amount of microparticles increased (data not shown).

3.4. Analytical performance of the biosensor

Having optimized the different parameters that may affect the current response, the modified electrode can be applied to the analytical APAP determination. Table 1 shows the linear range, detection limit and sensitivity (based on a signal-to-noise ratio

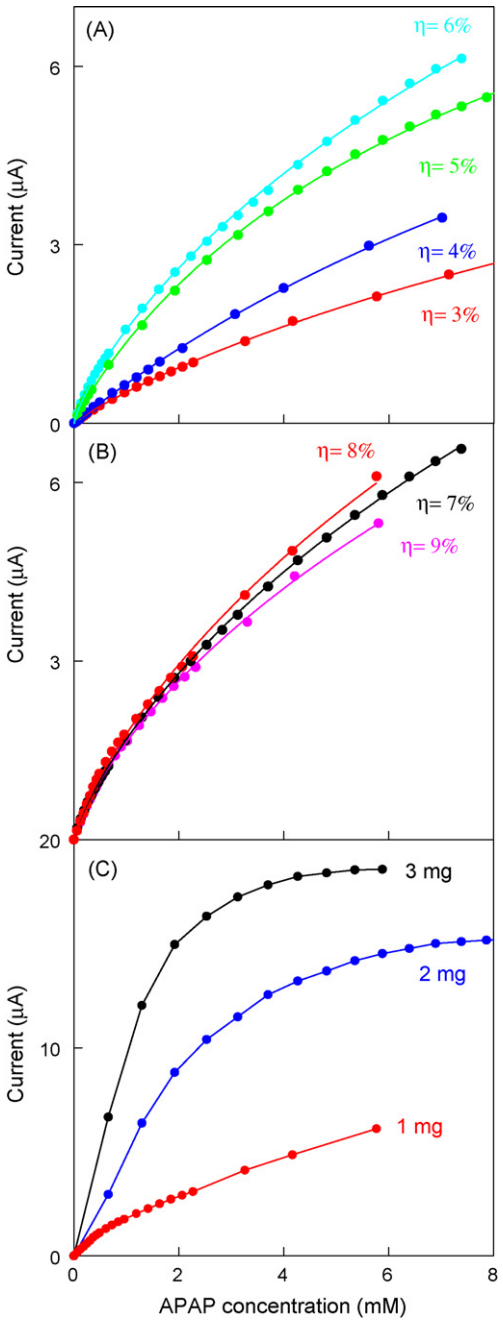

Fig. 1. (A and B) Influence of η on the biosensor response studied by calibration plot for APAP in stirred 50 mM PBS (pH 7.0) in the presence of 6.5 mM H_2O_2 at a potential of −0.1 V *vs.* SCE and 25 °C. The points correspond to experimental data while the lines correspond to data obtained by a non-linear regression analysis to Eq. (1). (C) Influence of the amount of microparticles placed on the electrode surface upon the current response. The weight of the microparticles was 1, 2 and 3 mg in the PAA microparticles with η = 8%.

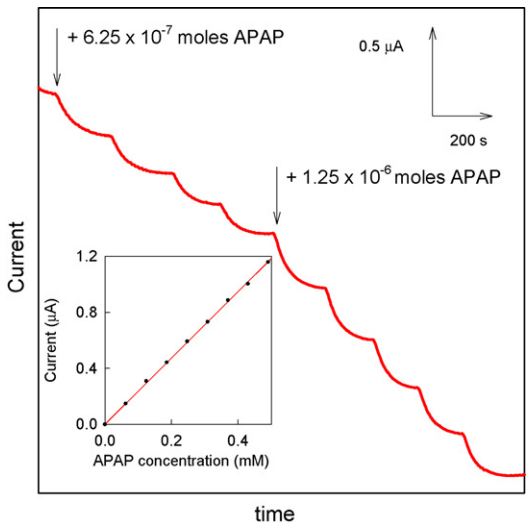

Fig. 2. Typical steady-state current response of the HRP-biosensor (η = 8%). Each addition corresponds to 6.25×10^{-7} or 1.25×10^{-6} mol of APAP, as indicated. Operating potential: −0.1 V *vs.* Ag/Cl. Experimental conditions as Fig. 1. The inset shows the linear response of the biosensor in the range 1.0×10^{-5} to 4.9×10^{-4} M APAP ($y = 0.010 + 2.336x$, $R^2 = 0.9995$).

equal to 3) of the different biosensors developed herein with different η. As previously seen, the maximum response was attained for the PAA microparticles with η = 8%. The biosensor linear range is wider than that reported between 1.96×10^{-5} and 2.55×10^{-4} M by Sima et al. (2008). Fig. 2 illustrates the current/time responses of the HRP-biosensor (η = 8%) due to the addition of aliquots of an APAP stock solution in an air-saturated buffer solution. The inset shows the linear range (the APAP concentration range in which a linear correlation with the current response was obtained) of the calibration plot in this case. RSD was 9.3% (n = 4) showing a better reproducibility than that obtained by other authors who found a RSD of 20% (Sima et al., 2008; Yu et al., 2006).

In order to test the applicability of this biosensor with real samples, interferences from some substances were examined under the optimum conditions. Sodium ascorbate, sodium citrate, salicylic acid, caffeine, D-mannitol and D-glucose were added to the cell to obtain final concentrations of 0.2 mM, but no response was detected. Furthermore, the signal for 0.1 mM APAP was the same in both the absence and the presence of the above substances, except ascorbate (data not shown). When ascorbate:APAP ratio exceed 1:1, it is able to affect the amperometric response by increasing the current signal. This could be due to the oxidation of ascorbate by HRP and the possible reduction of NAPSQI• by ascorbate. The good selectivity is attributed to the specificity of HRP and to the low working potential of −0.1 V used.

Another remarkable characteristic of this device is its easy preparation and the stability of HRP encapsulated in the microgels. The enzymatic activity of the freeze-dried microparticles was

Table 1
Values of kinetic parameters and analytical properties of the biosensor based on microgels with different η.

η (%)	Linear range (μM)	Detection limit (μM)	Sensitivity (mA M^{-1} cm^{-2})	K_M^{app} (mM)	Hill coefficient h	Extended range (μM)	Relative error $(4S_R/hR_{lim})$[a]
3%	38.0–728.2	12.0	16.94	5.19 ± 0.04	0.99 ± 0.03	38.0–8333.3	0.012
4%	17.0–728.2	5.1	21.50	5.00 ± 0.05	0.99 ± 0.02	17.0–7014.4	0.006
5%	5.8–657.9	1.7	46.85	5.83 ± 0.32	0.91 ± 0.02	5.8–8333.3	0.013
6%	5.6–331.1	1.7	69.25	8.85 ± 0.37	0.88 ± 0.01	5.6–7386.4	0.019
7%	17.8–396.8	5.3	67.54	8.89 ± 0.15	0.78 ± 0.01	17.8–7386.4	0.004
8%	10.2–490.2	3.1	74.90	9.05 ± 0.16	0.78 ± 0.03	10.2–5769.2	0.011
9%	10.2–490.2	3.1	63.68	13.81 ± 0.22	0.77 ± 0.02	10.2–5806.1	0.007

[a] R_{lim}: limiting rate value.

unalterable for at least 12 months indicating the goodness of the method to immobilize HRP. To characterize biosensor stability, it was stored in PBS at 4 °C, and the response against 60 μM APAP was recorded daily. We found that the biosensor exhibited 67.7% of the initial signal after 4 days and 32.3% after 7 days. This fact may be due to the H_2O_2-induced HRP inactivation (Arnao et al., 1990). The microparticles seems to constitute a protective environment for the biocomponent since our results represent a considerable improvement of biosensor stability with respect to data reported by other authors (Alonso-Lomillo et al., 2003). Biosensor lifetime relates with the time period that the biosensor is in contact with H_2O_2. If we consider the reproducibility obtained, we can see how this factor does not affect biosensor use.

The repeatability of the biosensor response was evaluated by performing 5 successive APAP measurements, yielding RSD = 3.5%; the variability of step length was 10.9% for five replicates. The reproducibility of the analytical response obtained with three different biosensors was analyzed, and resulted in RSD = 4.1%.

3.5. Kinetic behaviour of the biosensor

The HRP–H_2O_2–APAP system follows a ping-pong mechanism (Dunford, 1999) and, therefore, Lineweaver–Burk and Eadie–Hofstee plots of enzyme kinetics should result in straight lines. However, we obtained deviations from the linear behaviour that became higher as η increased (data not shown). This fact can be attributed to the influence on the kinetic parameters of immobilized enzymes of different factors such as inter- and intra-diffusion of substrates or products, steric and conformational effects, etc. If enzyme activity is low in comparison to the mass transfer rate, then the response is determined by the biocatalytical reaction, and the biosensor acts in the "kinetic regime". However if the overall process is determined by mass transport, then the biosensor acts in the "diffusion limitation regime" (Kulys, 2006).

Table 1 shows the apparent Michaelis–Menten constant (K_M^{app}) values obtained for the different PAA microparticles from the Eadie–Hofstee plots. Two clear regions were distinguished in the plots (data not shown): (a) a non-linear one at low substrate concentrations, showing a negative deviation of the expected linear behaviour predicted by the Eadie–Hofstee equation, which is very likely due to a diffusional control of the process; and (b) a linear region at relatively higher APAP concentrations, which is probably under kinetic control. The K_M^{app} values calculated from this latter region remained approximately constant for the microgels with $\eta < 5\%$. However for $\eta > 5\%$, K_M^{app} increased with a higher η due to the diffusional barrier imposed by the smaller pore size of these microparticles that hinder the affinity of HRP towards APAP.

It has been shown that, in those cases in which deviations from Michaelian behaviour are observed, the Hill equation, which is extensively used in enzyme kinetics, is applicable to calibration curves of both potentiometric and amperometric biosensors (Kurganov et al., 2001). The Hill equation has been rewritten as follows:

$$R = R_{\lim}\frac{\left(C/C_{0.5}\right)^h}{1+\left(C/C_{0.5}\right)^h} \quad (1)$$

where R is the biosensor response (current in this case), C is the analyte (APAP) concentration, R_{lim} is the value at $C \to \infty$ (maximum current), $C_{0.5}$ is the half-saturation concentration (at $R = R_{lim}/2$), and h is the Hill coefficient. At $h = 1$, the Hill equation turns into the classical Michaelis–Menten equation.

Data from Fig. 1A and B were fitted to Eq. (1) by non-linear regression and the h-values obtained are shown in Table 1. We may observe how $h \sim 1$ for the microparticles with $\eta < 5\%$ indicates kinetic control in these cases. However $h < 1$ for the PAA microparticles with $\eta > 5\%$ suggests that a diffusion of APAP and the product through the polymeric layer were the limiting steps in these cases. Notice that the Hill coefficients decreased when η increased. The calibration range of the different APAP biosensors developed herein can be extended using Eq. (1), as indicated in column 6 of Table 1. This range is wider than others previously reported in the literature (Messina et al., 2006; Sima et al., 2008; Yu et al., 2006). The analyte concentration (C_{APAP}) in a sample can now be determined from the calibration curve using the Hill equation once R_{lim}, $C_{0.5}$ and h are known:

$$C_{APAP} = \frac{C_{0.5}}{h\sqrt{R_{\lim}/R - 1}} \quad (2)$$

It has also been shown that the relative error in the measurement of the analyzed substrate concentration is minimal at $C = C_{0.5}$ and equal to $4S_R/hR_{lim}$. These values were calculated for the curves shown in Fig. 1A and B by using the parameters yielded by the non-linear regression. The data obtained in this way are shown in Table 1 (column 7).

To check the applicability of Eq. (2), three replicates of the calibration plot for the microparticles with $\eta = 8\%$ were performed, and the following mean values were obtained: $\overline{h} = 0.82 \pm 0.01$ and $\overline{R_{\lim}} = 34.5 \pm 2.67$ μA. These low standard deviation values obtained show the good reproducibility of h and R_{lim}; therefore the Hill equation can be effectively used to measure APAP in real samples.

3.6. APAP quantification in commercial formulations

To check the applicability of the biosensor in pharmacological samples, the proposed method was satisfactorily applied to the APAP determination in three commercial pharmaceutical formulations (tablets). C_{APAP} in the samples calculated by Eq. (2) were compared to those obtained by HPLC analysis (reference method), and the results are shown in Table 2. The R.S.D. values were below 4.1%, revealing good biosensor precision.

Table 2
Analytical results of the three APAP commercial formulations with the biosensor and the HPLC method.

Sample	[APAP] (mM) Reference method (HPLC)	[APAP] (mM) Present method	R.S.D. (%)[a]
No. 1	0.109 ± 0.002	0.124 ± 0.004	2.9
No. 2	0.107 ± 0.002	0.128 ± 0.003	2.1
No. 3	0.095 ± 0.001	0.112 ± 0.005	4.1

Stock solutions were diluted to give final APAP concentrations of 0.1 mM. Values are expressed as the mean of three replicates ± standard deviation.
[a] R.S.D.: relative standard deviation.

3.7. The diffusion coefficients of APAP in the microgels

A typical amperometric biosensor presents three regions: (a) the enzyme layer where both the enzymatic reaction and mass transport by diffusion take place, (b) a diffusion limiting region where only diffusion takes place, and (c) a convective region where the analyte concentration remains constant (Baronas and Ivanauskas, 2004). The mass transfer of the analyte molecules towards the electrode surface from the bulk solution is one of the most important factors that affects biosensor response, mainly when a biocatalyst is immobilized inside a porous support like PAA microgels (Yankov, 2004). Obviously, the pore size of the microparticles remarkably affects the diffusion component, as we have just seen. For this reason, the study of the apparent diffusion coefficients (D^{app}) may prove very interesting for the characterization of biosensor output.

The Cottrell equation describes the evolution of the current, I, along a chronoamperogram, t, as a function of the diffusion coeffi-

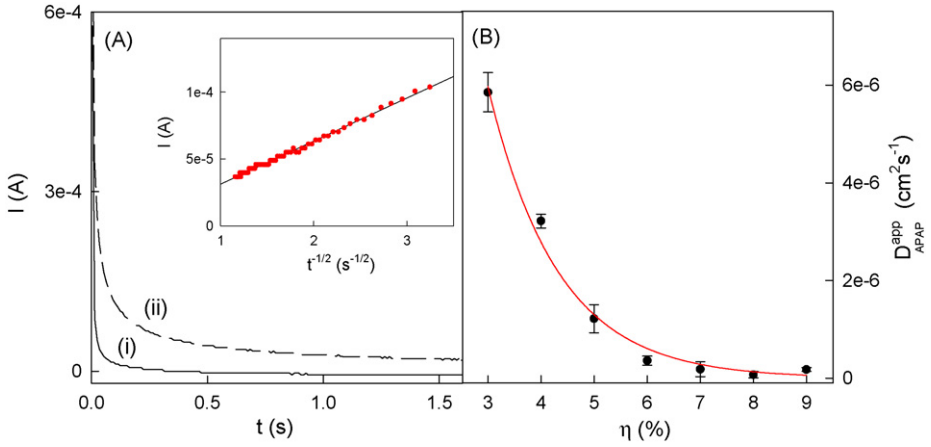

Fig. 3. (A) Potential step background current comparison: (i) background signal for the modified electrode in buffer; (ii) signal of 25.0 mM APAP solution. The inset shows the data corrected by the blank signal *vs.* $t^{-1/2}$ (Cottrell plot). (B) Influence of cross-linking on D^{app}_{APAP} derived using the Cottrell equation. The potential used was +0.6 V. Each point represents the average of three different experiments.

cient, D (Suárez et al., 2005) in a "diffusion controlled" process:

$$I = \frac{nFAD^{1/2}C}{\pi^{1/2}t^{1/2}} \quad (3)$$

where n is the number of electrons involved in the process, F the Faraday constant, A the area of the electrode, C the bulk concentration of the reducible analyte, and t the time. From this equation, D^{app} for APAP (D^{app}_{APAP}) can be calculated. Fig. 3A shows a Cottrell plot for the typical data obtained from a potential step experiment. A linear relationship was found in the plot I *vs.* $t^{-1/2}$ in the region 0.2–0.6 s (Fig. 3A, inset). From the slope, D^{app}_{APAP} was calculated using the Cottrell equation for the microgels with different η, and the results can be seen in Fig. 3B. D^{app}_{APAP} was also measured in the absence of microgels and the data obtained were $7.7 \pm 0.2 \times 10^{-6}$ cm^2 s^{-1} for the electrode covered with the membrane, and $1.5 \pm 0.1 \times 10^{-5}$ cm^2 s^{-1} for the bare electrode. These results indicate that the diffusional barrier imposed by the dialysis membrane should also be considered since it influences biosensor response.

Note that D^{app}_{APAP} is strongly dependent on increasing pore size as η decreases. The data of Fig. 3B fit ($R = 0.9894$) an uniexponential equation well:

$$D^{app}_{APAP} = Ae^{-B\eta} \quad (4)$$

where $A = 5.9 \times 10^{-5}$ cm^2 s^{-1} and $B = 0.8$. This behaviour is attributed to the water content inside the PAA microparticles which is higher at a low η. Thus, the microenvironment of the entrapped enzyme in the PAA microgels with a low η is similar to that in solution, and the diffusional barriers are lower as η decreases. This result may be useful in the mathematical modelling of HRP-biosensors and bioreactors with enzymes immobilized within microgels.

4. Conclusions

In short, the HRP-PAA-based biosensor has been successfully used for amperometric APAP determination in standard laboratory and real pharmaceutical samples without the need of pre-treatment steps. The entrapment of HRP in PAA microgels offers an excellent protective environment for the long storage of microparticles, great simplicity and low cost in their preparation compared with other typical protocols reported for preparing modified electrodes. The main experimental variables, namely, the cross-linking degree of PAA microgels, H_2O_2 concentration and enzyme load, have been optimized. No correlation of pore size and H_2O_2-induced deactivation rate was found. The apparent diffusion coefficients of APAP decay exponentially when pore size decreases. The biosensor shows very good catalytic activity with good linearity for APAP determination over a range of 1.0×10^{-5} to 4.9×10^{-4} M. We have shown that the calibration range can be extended using the Hill equation because of the biosensor's very good reproducibility. Although biosensor stability is affected by the progressive action of H_2O_2 on HRP, PAA microparticles exhibit a protective effect on the biocatalyzer, which clearly improves stability of the biosensor with respect to other approaches used in the literature (Alonso-Lomillo et al., 2003). This allows obtaining better repeatability and reproducibility parameters for this biosensor. Furthermore the biosensor is very specific to APAP and shows high sensitivity. For all these reasons, we consider that this biosensor offers an inexpensive, fast and reliable method for efficient APAP determination in quality control applications in the pharmaceutical industry, as well as possible medicinal and toxicological applications.

Acknowledgements

The authors acknowledge financial support from the UCM-BSCH program for "Consolidation of Research Groups" (Group 911033, grant GR58/08), from the COST Action D43 and from the Regional Ministry of Science and Technology (JCCM, Spain) (PAI-05-036 and PAI-08-0175-8618). M.I.G.S. is a predoctoral fellowship from JCCM associated with project PAI-05-036. The authors are most indebted to Prof. F. Martínez-Ortiz from the University of Murcia (Spain) for his useful advice during this work.

Appendix A. Supplementary data

Supplementary data associated with this article can be found, in the online version, at doi:10.1016/j.bios.2010.03.024.

References

Alonso-Lomillo, M.A., Kauffmann, J.M., Arcos-Martínez, M.J., 2003. Biosens. Bioelectron. 18, 1165–1171.
Al-Zoubi, N., Koundourellis, J.E., Malamataris, S., 2002. J. Pharm. Biomed. Anal. 29, 459–467.
Arnao, M.B., Acosta, M., Del Río, J.A., Varón, R., García-Cánovas, F., 1990. Biochim. Biophys. Acta.: Prot. Struct. Mol. Enzymol. 1041, 43–47.
Bard, A.L., Faulkner, R., 2001. Electrochemical Methods: Fundamentals and Applications, second ed. John Willey & Sons, New York.
Barman, T.E., 1969. Enzyme Handbook, vol. 1, first ed. Springer-Verlag, New York.
Baronas, R., Ivanauskas, F., 2004. J. Math. Chem. 35, 199–213.
Bessems, J.G.M., DeGroot, M.J., Baede, E.J., TeKoppele, J.M., Vermeulen, N.P.E., 1998. Xenobiotica 28, 855–875.
Dunford, H.B., 1999. Heme Peroxidases, first ed. John Wiley & Sons, New York.

Easwaramoorthy, D., Yu, Y.C., Huang, H.J., 2001. Anal. Chim. Acta 439, 95–100.
Espinosa-Bosch, M., Ruiz-Sánchez, A.J., Bosch-Ojeda, C., 2006. J. Pharm. Biomed. Anal. 42, 291–321.
Fatibello, O., Lupetti, K.O., Vieira, I.C., 2001. Talanta 55, 685–692.
González-Sánchez, M.I., Manjabacas, M.C., García-Carmona, F., Valero, E., 2009. Chem. Res. Toxicol. 22, 1841–1850.
Harwood, G.W.J., Pouton, C.W., 1996. Adv. Drug Deliv. Rev. 18, 163–191.
Hervás-Pérez, J.P., Sánchez-Paniagua López, M., López-Cabarcos, E., López-Ruiz, B., 2006. Biosens. Bioelectron. 22, 429–439.
Josephy, P.D., 2005. Drug. Metab. Rev. 37, 581–594.
Kulys, J., 2006. Nonlinear Anal.: Model. Control 11, 385–392.
Kurganov, B.I., Lobanov, A.V., Borisov, I.A., Reshetilov, A.N., 2001. Anal. Chim. Acta 427, 11–19.
Lee, W.M., 2007. Hepatology 46, 966–970.
Marin, A., García, E., García, A., Barbas, C., 2002. J. Pharm. Biomed. Anal. 29, 701–714.
Messina, G.A., De Vito, I.E., Raba, J., 2006. Anal. Chim. Acta 559, 152–158.
Miner, D.J., Rice, J.R., Riggin, R.M., Kissinger, P.T., 1981. Anal. Chem. 53, 2259–2283.
Mohamed, F.A., AdbAllah, M.A., Shammat, S.M., 1997. Talanta 44, 61–68.
Nazari, K., Mahmoudi, A., Khosranech, M., Haghighian, Z., Moosavi-Movahedi, A.A., 2009. J. Mol. Catal. B: Enzym. 56, 61–69.
Nelson, D.P., Kiesow, L.A., 1972. Anal. Biochem. 49, 472–478.
Rubio-Retama, J., López-Ruiz, B., López-Cabarcos, E., 2003. Biomaterials 24, 2965–2973.
Rubio-Retama, J., López-Cabarcos, E., López-Ruiz, B., 2005. Talanta 68, 99–107.
Sánchez-Paniagua López, M., Tamimi, F., López-Cabarcos, E., López-Ruiz, B., 2007. Electroanal 19, 370–378.
Sima, V., Crista, C., Lapadus, F., Marin, I.O., Marian, A., Sandulescu, R., 2008. J. Pharmaceut. Biomed. 48, 1195–1200.
Suárez, I.J., Otero, T.F., Márquez, M., 2005. J. Phys. Chem. 109, 1723–1729.
Valero, E., Varón, R., García-Carmona, F., 2002. Biol. Chem. 383, 1931–1939.
Valero, E., Carrión, P., Varón, R., García-Carmona, F., 2003a. Anal. Biochem. 318, 187–195.
Valero, E., Varón, R., García-Carmona, F., 2003b. Arch. Biochem. Biophys. 416, 218–226.
Vaughan, P.A., Scott, L.D.L., McAleer, J.F., 1991. Anal. Chim. Acta 248, 361–365.
Wangfuengkanagul, N., Chailapakul, O., 2002. J. Pharm. Biomed. Anal. 28, 841–847.
Yankov, D., 2004. Enzyme Microb. Tech 34, 603–610.
Yu, D., Domínguez-Renedo, O., Blankert, B., Sima, V., Sandulescu, R., Arcos, J., Kauffmann, J.M., 2006. Electroanal 18, 1637–1642.
Zhao, S., Bai, W., Yuan, H., Xiao, D., 2006. Anal. Chim. Acta 559, 195–199.